

## Nonthermal effects on hydrogen-line profiles

R. W. Lee and W. L. Morgan

Lawrence Livermore National Laboratory (L-23), University of California, P.O. Box 808, Livermore, California 94550

(Received 18 January 1985)

Experimentally determined level populations of hydrogen excited states from a low-density Z pinch are used as initial conditions in a simulation to derive electron-velocity distributions. These velocity distributions show excess electrons in the high velocity end of the distribution when compared to a Maxwellian velocity distribution. The non-Maxwellian velocity distributions are used to find the nonequilibrium structure factors which are a main component in the plasma line broadening of hydrogen lines. The line profiles generated using the structure factors show plasmon satellites on the wings of the Balmer- $\alpha$ - and - $\beta$ -line profiles.

### I. INTRODUCTION

The occurrence of non-Maxwellian velocity distributions in laboratory plasmas has been documented for a number of years. The possible sources of non-Maxwellian velocity distributions have been selective optical pumping,<sup>1</sup> particle-beam injection,<sup>2</sup> and, more recently, the electron velocity distribution relaxing to steady state in a hydrogen-recombination Z pinch which has a substantial overpopulation of excited states relative to local thermal equilibrium (LTE).<sup>3</sup> The latter work on the hydrogen-recombination plasma will be the primary focus of the work presented below.

One reason for the interest in non-Maxwellian velocity distributions is that spectroscopic observables can be altered by these distributions. The electron plasma frequency emission, which is in the microwave region in the low-density laboratory plasmas we consider here, will be enhanced when there is an excess of electrons in the high-energy part of the distribution.<sup>4</sup> Also, the laser-light scattering signal will be modified,<sup>4</sup> and the enhanced plasmon level will couple to atomic emitters and cause satellites on the spectral line wings.<sup>5</sup>

In the previous work on plasma satellite lines, the increased electron plasma wave activity of the plasma was due to turbulence. In this paper we show that the possibility of observable effects may arise in the quiescent afterglow where turbulence is a negligible factor. These results, which show plasma satellites can arise from a nonturbulent system, suggest that this may be a method of probing for non-Maxwellian velocity distributions when the deviations occur on the high-energy end of the distribution. These deviations are difficult to determine because the number of electrons in the tail at  $E_i$  is many orders of magnitude below the maximum when  $E_i \gg K_B T$ , the thermal energy.

To assist in clarifying our procedure, we will now outline the procedure employed. First, using the *measured* values of the excited-state populations, temperature and densities from the recombination phase of a hydrogen Z pinch we find that the first and second excited states have LTE departure coefficients which are much greater than 1.<sup>6</sup> Next, we use the observed level populations in a simu-

lation which determines the velocity distribution that is self-consistent with these populations,<sup>1</sup> and it is found that this distribution has an enhanced high-velocity tail.<sup>3</sup> Then a formulation which can handle nonthermal systems is employed to obtain the structure factor  $S(\kappa, \omega)$ .<sup>7</sup> The structure factor, which is central to the radiative properties of the plasma, can then be used to determine the electron plasma wave contributions, the scattered signal,<sup>4</sup> and the effects on the spectral line profiles.<sup>5,7</sup>

### II. EXPERIMENTAL RESULTS

Since the starting point of the theoretical investigation is the experimental level populations, we present a brief description of those results. The experimental results are taken from the work of the Spectroscopy Group at Imperial College.<sup>6</sup> In this work a recombination plasma has been characterized by using Thompson scattering, interferometry, optical pumping, and emission spectroscopy. The plasma phase we consider here are many microseconds after the peak current and the electron density is on the order of  $10^{14} \text{ cm}^{-3}$  with an electron temperature about 0.4 eV. To emphasize the deviations in the measured level populations we use the departure coefficient  $B_i$ , defined by the equation

$$B_i = n_i^{\text{expt}} / n_i^{\text{LTE}},$$

where  $n_i^{\text{expt}}$  is the experimentally determined population of level  $i$  and  $n_i^{\text{LTE}}$  is the population assuming that the level  $i$  is in LTE with the experimentally determined ion populations at the experimental temperature. It is found that the  $B_i$  are greater than 1000 for the first excited state of  $n_i$ .

This overpopulation is large and will be the source of the non-Maxwellian velocity distribution. The process for producing the non-Maxwellian is for electrons to depopulate the  $n_2$  state through collisions giving 10.2 eV to the electrons. Due to the low temperatures  $\sim 0.4$  eV these electrons will not be effectively thermalized and a bump on the tail of the velocity distribution is formed. The exact phase in the recombination when the temperature and density drop low enough to allow this to happen has been

determined in a previous work and it should be noted that, indeed, the high-velocity tail excess grows at late time.<sup>3</sup>

### III. THEORY

#### A. Velocity distribution

The time scales for decay of the level populations and the electron density are on the order of  $10 \mu\text{s}$  while the time scales for the electron-electron and the hydrogen-electron interactions are many orders of magnitude lower ( $< 10 \text{ ns}$ ). Thus, an appropriate model to study the velocity distribution is to assume that the level populations are a fixed initial condition and that the velocity distribution  $f(v)$  relaxes to a steady state consistent with these level populations.

The level populations we use in the simulation are

$$n_1 = n_{\text{gas}} - n_{\text{ion}} - \sum_{i>1} n_i,$$

$$n_{2,3} = n_{2,3}^{\text{expt}},$$

$$n_{i>3} = n_i^{\text{LTE}},$$

where  $n_{\text{gas}}$  is the hydrogen gas density and  $n_{\text{ion}}$  is the ion density which is equal to the experimentally determined electron density  $n_E$ .

The simulation is described in detail in Bach *et al.*<sup>3</sup> Briefly, we solve the Boltzmann equation

$$\left[ \frac{\partial}{\partial t} + \mathbf{V}_r \cdot \nabla + \frac{\mathbf{f}}{m} \cdot \nabla_v \right] f(v, r, t) = \left[ \frac{\partial f}{\partial t} \right]_{\text{collisions}} \\ \equiv \partial f|_c,$$

where we assume that the system is spatially homogeneous. A two-term Legendre expansion of the form

$$f(v) = f_0(v) + \frac{\mathbf{V}}{V} \cdot \mathbf{f}_1(v)$$

is employed.

The  $\partial f|_c$  term is the collisional term and in the simulation includes the momentum transfer between free electrons, and inelastic and superelastic collision between bound and free electrons. The electron energy spectrum is separated into 200 bins with the discrete energy bound electrons included as the lowest energy bins. In this way both bound- and free-electron energy distributions are calculated in a unified manner.

In the present case, we calculate the velocity distribution for the plasma-condition electron density  $n_e = 2 \times 10^{14} \text{ cm}^{-3}$  and electron temperature  $T_e = 0.4 \text{ eV}$ . In Fig. 1, we show the results of the calculations of the velocity distribution represented as  $v^3 f(v)$ . The abscissa is a logarithmic scale and the ordinate is energy in eV. The dotted line represent the Maxwellian at a temperature of 0.4 eV and the solid line is the result of the simulation. Note that the simulation shows a bump on the high-velocity tail and this starts at  $\sim 7 \text{ eV}$  which represents the diffusion in energy of the predominant 10.2 eV from superelastic collisions between hydrogen levels 2 to 1.

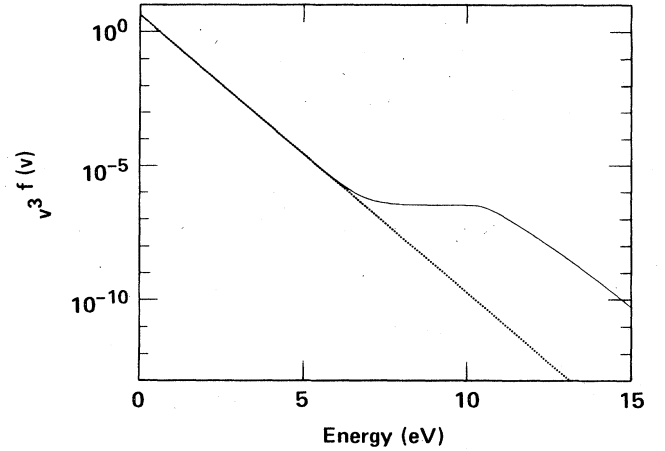


FIG. 1. Velocity distribution plotted as  $v^3 f(v)$  for the plasma conditions  $N_e = 2 \times 10^{14} \text{ cm}^{-3}$ ,  $T_e = 0.43 \text{ eV}$  vs the energy in eV. The solid line is the distribution determined by the simulation; dotted line is the Maxwellian shown for comparison.

The low-energy end of the distribution is the same as the Maxwellian and indicates *a posteriori* that our use of the temperature to derive an initial estimate of  $f(v)$  is valid.

#### B. Formulation of the structure factor

Since the high-velocity tail of the distribution can be a source of enhanced plasma-wave emission, we next study the radiative properties. As a first step in the evaluation of the radiative properties, we need to evaluate the structure factor  $S(\kappa, \omega)$  which is the Fourier transform of the density-density correlation function. Here  $\kappa$  is the wave vector and  $\omega$  is the frequency.

Following the work of Tidman and Dupree,<sup>4</sup> we obtain the standard form of the  $S_{ee}(\kappa, \omega)$ , the electron-electron  $S(\kappa, \omega)$ . However, we obtain the standard form with modified definitions, that is,

$$S_{ee}(\kappa, \omega) = \frac{\pi}{\kappa} \frac{\tilde{F}_e(\omega/\kappa) |1 + G_I|^2 + \tilde{F}_I(\omega/\kappa) |G_e|^2}{|1 + G_e + G_I|^2},$$

where the subscripts  $e$  and  $I$  refer to the electron and ion subsystems, respectively. Here the  $\tilde{F}$  and  $G$  are defined in terms of the velocity-distribution function  $f$ , the thermal velocity  $v_{\text{th}}$ , and the Debye wave number  $\kappa_D$ :

$$\kappa = (4\pi n_e e^2 / k_B T)^{1/2}, \quad v_{\text{th}} = (2k_B T / m)^{1/2},$$

$$F(x) = \frac{1}{v_{\text{th}}} \int_{k/v_{\text{th}}}^{\infty} dz z H(z), \quad H(y) = 2\pi v_{\text{th}}^3 f(y),$$

$$G_{e,I} = G_{e,I}^{\text{real}} + iG_{e,I}^{\text{imag}},$$

$$G_{e,I}^{\text{real}} = x^2 \left[ \int_0^{\infty} H(z) dz - \frac{1}{2} \int \frac{H(z)}{1-z/y} \right],$$

$$G_{e,I}^{\text{imag}} = \frac{\pi}{2} x^2 y H(y)$$

with the dimensionless units  $y$  and  $x$  defined as

$$x = \kappa_D / \kappa, \quad y = \omega / (\kappa v_{th}).$$

These equations will reduce to the usual description when a Maxwellian velocity distribution is employed for  $f(v)$ .

### 1. Results for light scattering

The structure factor  $S_{ee}$  is the quantity measured when one irradiates a plasma with a laser of wavelength  $\lambda$  and observes the signal at some angle  $\theta$  relative to the incident laser. Depending on the scattered laser wave number relative to the Debye wave number, one will sample collective modes or particle modes. The relevant parameter is

$$\alpha = \kappa_D / \kappa = 1.58 \times 10^{-12} \lambda N_e / T_e (1 - \cos\theta)^{1/2},$$

where  $T_e$  is measured in eV. We find that in the particle regime, when  $\alpha < 1$ , the scattered signal is the same for the non-Maxwellian  $f(v)$  in Fig. 1, and the Maxwellian  $f(v)$  with the temperature  $T_e$ . However, in the limit of  $\alpha > 1$ , when the collective electron plasma waves mode will give a scattering contribution, we obtain an enhanced signal from the non-Maxwellian  $f(v)$  when compared to the Maxwellian case. In Fig. 2 we show the  $S_{ee}$  result for scattering into  $\pi/36$  which gives an  $\alpha$  of 4. Figure 2 illustrates enhanced plasma-wave contributions, as indicated in the inset where the regime about the plasma frequency is expanded and one can observe the effect. This can be interpreted as arising from the excess of high-velocity electrons which contribute to the electron wave emission. There is the possibility of determining the high-velocity electrons by scattering. However, since scattering in the collective regime is usually complicated by signal-to-noise problems, we could approach the problem by measuring the plasma emission in the region about  $\omega_{pe}$ .<sup>4</sup> The difficulty with this approach is that the collective emission from the plasma is only a small part of the total emission. This is discussed below.

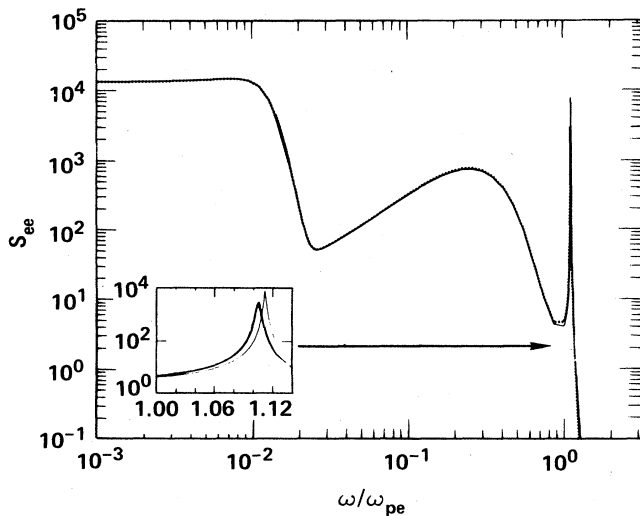


FIG. 2. Logarithm of  $S_{ee}(\kappa, \omega)$  vs the logarithm of the frequency in units of the electron-plasma frequency  $\omega_{pe}$ . Inset shows a detail of the collective contributions. Solid line is the non-Maxwellian. This is for a scattering angle of  $\pi/36$ .

### 2. Results for the emissivity and shift-and-width operator

The emissivity of the plasma can be defined in terms of  $S_{ee}(\kappa, \omega)$ , i.e.,

$$\epsilon(\omega) \propto \int d\kappa S_{ee}(\kappa, \omega).$$

This function is closely related to the shift-and-width operator  $H(\omega)$  in the formulation of spectral line broadening, and since the possibility that non-Maxwellian velocity distributions can produce satellites on the wings of the spectral line profile has been previously investigated,<sup>5</sup> we use the integral of  $S_{ee}$  for both cases.

To connect the formulation of  $S_{ee}(\kappa, \omega)$  to the line broadening of atoms in a plasma, we refer to previous theoretical development.<sup>7</sup> The formulation of the intensity  $I(\omega)$  from spectral line broadening in plasmas can be written schematically as

$$I(\omega) \sim \int P(\epsilon) d\epsilon [\Delta\omega(\epsilon) + iH(\omega)]^{-1},$$

where  $P(\epsilon)$  is the ion microfield,  $\Delta\omega(\epsilon)$  is the Stark field-dependent transition energy. Here

$$\text{Re}H(\omega) \sim \int_0^{\kappa_{\max}} d\kappa S_{ee}(\kappa, \omega),$$

$$\text{Im}H(\omega) = \frac{1}{\pi} \int \frac{\text{Re}H(\omega')}{\omega - \omega'} d\omega'.$$

The evaluation of the shift-and-width operator requires further restriction imposed by the theoretical development. First, we exclude those contributions from strong collisions by using a  $\kappa_{\max}$  cutoff. These are included in a "strong-collision" term which is evaluated by estimating those collisions which violate unitarity.<sup>7</sup> Further, we will use the standard approximation of quasistatic ions and dynamic electrons, we then have for  $S_{ee}$

$$S_{ee}(\kappa, \omega) = \frac{\pi}{\kappa} \tilde{F}_e(\omega/\kappa) / |1 + G_e|^2.$$

The result for the evaluation of the shift-and-width operator is shown in Fig. 3. The  $\text{Re}H(\omega)$  is shown as a solid

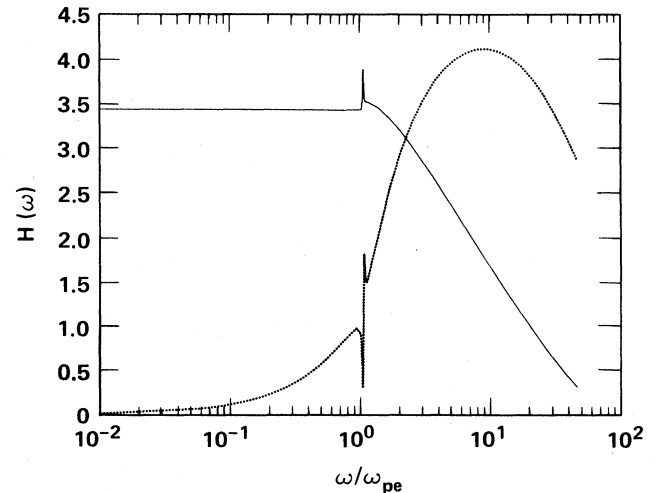


FIG. 3. Shift-and-width operator  $H(\omega)$  vs the logarithm of the frequency in units of  $\omega_{pe}$ . Solid line is the real part  $\text{Re}H(\omega)$ , and dotted line is the imaginary part  $\text{Im}H(\omega)$ .

line while  $\text{Im}H(\omega)$  is a dotted line. The abscissa is as in Fig. 2 with the region of interest being about the electron plasma frequency. The bump on the  $\text{Re}H(\omega)$  near  $\omega_{pe}$  is due to the enhanced plasma-wave contributions. In a thermal system the contribution at this frequency is negligible. Further, note that the  $\text{Im}H(\omega)$  shows a large effect due to the wave contributions.

The emissivity is essentially the  $\text{Re}H(\omega)$ , however, the cutoff  $\kappa_{\text{max}}$  will be much larger. The affect of this increased cutoff is that the particle contributions to  $\text{Re}H(\omega)$  will be increased greatly while the wave contributions will be the same as in Fig. 3. This is because the plasma waves do not exist for  $\kappa > \kappa_D$  and our cutoff  $\kappa_{\text{max}}$  will include all the wave contributions. This indicates that the relative emissivity increase at  $\omega_{pe}$  will be a very small part of the total emissivity and direct measurements of the excess electrons in high-velocity tail would be complicated.

#### IV. LINE PROFILES

To study the possible affect on the line profile of the nonthermal velocity distribution, we study the hydrogen Balmer- $\alpha$  and - $\beta$  transition. In Figs. 4 and 5, we have plotted the results of relative intensity versus the frequency separation from line center in units of  $\omega_{pe}$ . The solid curves are the result derived using the non-Maxwellian  $f(v)$  while the dotted line used the Maxwellian. The inset shows an expanded view of the region about  $\Delta\omega_{pe}$ . In Figs. 4 and 5 the Stark quasistatic ion and electron collision broadening are included. The Doppler broadening is  $0.06\omega_{pe}$ .

In Figs. 4 and 5, we see a very small bump around the  $\Delta\omega_{pe}$ . This is due to enhanced plasma waves and, thus, follows the shape of the  $\text{Re}H(\omega)$ . That is, since  $\Delta\omega_{pe}$  is far from line center the  $\text{Im}H(\omega)$  in the function  $\Delta\omega_{pe} + \text{Im}H(\omega)$  is not large enough to produce an effective zero. The inset in these figures shows that we have

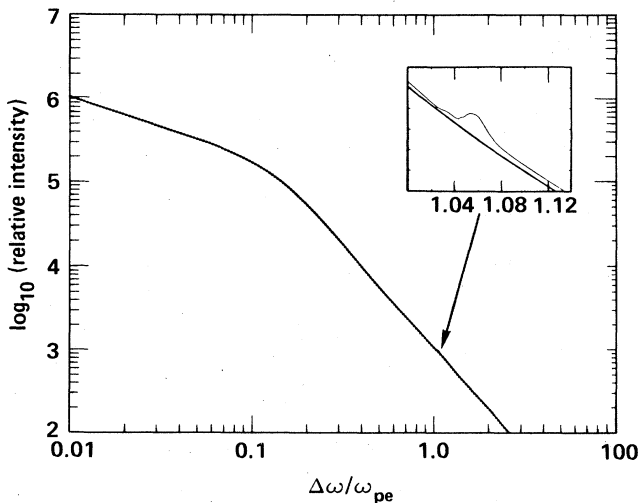


FIG. 4. Logarithm of the line profile for the 3-2 transition in hydrogen vs the frequency separation from line center in units of  $\omega_{pe}$ . Inset shows the region about the  $\Delta\omega_{pe}$  on a linear scale. Conditions are as in Fig. 1.

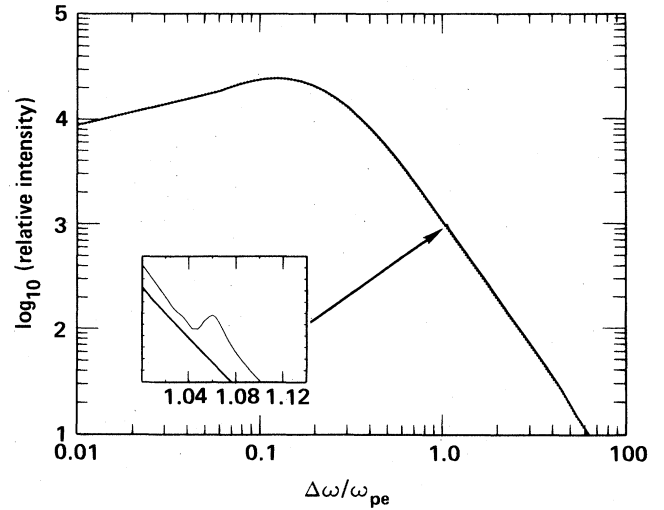


FIG. 5. Logarithm of the line profile for the 4-2 transition in hydrogen vs the frequency separation from line center in units of  $\omega_{pe}$ . Inset shows the region about the  $\Delta\omega_{pe}$  on a linear scale. Conditions are as in Fig. 1.

plasmon bumps arising from a quiescent nonthermal plasma. In the case of  $H_\beta$  the 4 to 2 transition shows an experimental possibility since the plasmon "bump" is a factor of  $\sim 20$  down on the peak intensity, and spectroscopic methods exist which could resolve this feature using Doppler-free spectroscopy.

#### V. COMMENTS

We have shown the existence of excess electrons in the high-energy tail of the  $f(v)$  which arise when the velocity distribution is allowed to relax to *measured* level populations in the recombination phase of a hydrogen Z pinch. The possibility of measuring the existence of this high-velocity tail excess has been addressed. In summary, we could perform laser scattering in the particle regime, which would require scattering from a part of the distribution that is more than 7 orders of magnitude below the peak. Second, scattering in the collective regime could be performed where the scattering angle is small. This would require both measurements about the  $\omega_{pe}$  region and at frequencies where the thermal and nonthermal signals are expected to be equivalent. Third, there is the possible use of the enhanced collective emission at the  $\omega_{pe}$  which is limited by the fact that the collective emission is only a small fraction of the total emission. Finally, the use of the plasma satellite, on the wings of spectral lines, has been proposed. In this case, the possibility of performing high-precision laser spectroscopy provides a method by which the calculations in this work can be checked.

As a final comment, it should be pointed out that the theoretical analysis contains a number of deficiencies. First, the simulation does not contain a fully self-consistent approach to the plasma wave producing high-velocity electrons. In a more complete formulation, the damping of these waves would have to be included in the

numerical simulation. Second, the inclusion of collisions in the formulation of the  $S(\kappa, \omega)$  will potentially broaden out the collective modes.<sup>8</sup> Third, it is of interest to work on the helium-forbidden lines where plasma satellites couple more favorably to the atom. To perform these calculations, we need experimental data on the level populations in a quiescent helium plasma of the same high quality as the hydrogen populations used in the present study.

#### ACKNOWLEDGMENTS

We would like to thank the experimentalists of the Spectroscopy Group at Imperial College of Science and Technology, University of London, for the experimental information contained in this paper. This work was performed under the auspices of the U.S. Department of Energy by Lawrence Livermore National Laboratory under Contract No. W-7405-Eng-48.

---

<sup>1</sup>W. L. Morgan, *Appl. Phys. Lett.* **42**, 790 (1983).

<sup>2</sup>N. Peyraud, *Phys. Fluids* **21**, 1490 (1978).

<sup>3</sup>T. Bach, R. W. Lee, and W. L. Morgan (unpublished).

<sup>4</sup>D. A. Tidman and T. H. Dupree, *Phys. Fluids* **8**, 1860 (1965).

<sup>5</sup>W. Chappell, J. Cooper, and E. W. Smith, *J. Quant. Spectrosc. Radiat. Transfer* **10**, 1195 (1970); R. W. Lee, *J. Phys. B* **12**,

1165 (1979).

<sup>6</sup>D. D. Burgess, V. P. Myerscough, C. H. Skinner, and J. M. Wards, *J. Phys. B* **13**, 1675 (1980).

<sup>7</sup>J. W. Dufty, *Phys. Rev.* **187**, A305 (1969); R. W. Lee, *J. Phys. B* **12**, 1129 (1979).

<sup>8</sup>R. Cauble and D. W. Boercker, *Phys. Rev. A* **28**, 944 (1983).